

# Phase separation in doped Mott insulators

Chuck-Hou Yee\* and Leon Balents

*Kavli Institute for Theoretical Physics, University of California Santa Barbara, CA 93106, USA*

(Dated: May 10, 2019)

Motivated by the commonplace observation of Mott insulators away from integer filling, we construct a simple thermodynamic argument for phase separation in first-order doping-driven Mott transitions. We show how to compute the critical dopings required to drive the Mott transition using electronic structure calculations for the titanate family of perovskites, finding good agreement with experiment. The theory predicts the transition is percolative and should exhibit Coulomb frustration.

The Mott transition is a pervasive and complex phenomena, observed in many correlated oxide systems [1]. It comes in two varieties: the bandwidth-controlled transition at half-filling, tuned by the ratio of the on-site Coulomb repulsion  $U$  and band-width  $W$ , and the filling-controlled transition, tuned by electron doping  $x$  away from half-filling. Theoretically, Mott insulators exist only at half-filling: with one electron per site, hoppings necessarily create empty and doubly-occupied sites which are heavily penalized by  $U$ . Introducing a finite charge density allows carriers to move without incurring the on-site Coulomb cost, destroying the Mott insulator [2]. However, experiments in a wide variety of transition metal oxides show that the critical doping  $x_c$  needed to destroy insulating transport is not zero, but rather a substantial fraction of unity [3], ranging from 0.1 in the nickelates [4] to 0.5 in the vanadates [5]. Systematic variations of  $x_c$  with bandwidth also argue that it is an intrinsic quantity [6], and motivate the search for mechanisms independent of disorder or coupling to lattice vibrations for insulating behavior away from half-filling.

The scenario of doping a Mott insulator has been heavily studied by a variety of techniques [7–10]. For the classic case of a square lattice, basic issues such as whether the Mott transition is first [11, 12] or second [13–15] order, the specific parameter regimes and underlying mechanisms of phase separation [16–20], and the structure of the inhomogeneous phases [21–23] have been actively researched, with results dependant on the precise model considered. We take a different approach: we assume the *bandwidth*-controlled Mott transition is first-order and deduce its implications by constructing a simple thermodynamic description. We predict that the filling-controlled transition is first order as a consequence, implying that phase separation occurs and the critical doping scales as  $x_c \sim \sqrt{U - U_c}$ , where  $U_c$  defines the critical  $U$  for the bandwidth controlled transition. We show how to compute  $x_c$  in electronic structure calculations [24], using the rare earth titanates [25, 26] as a prototypical example.

*Thermodynamics* – We construct a theory of the Mott transition by connecting the bandwidth- and filling-controlled transitions. By assuming the former transition is first-order (which covers the majority of cases observed

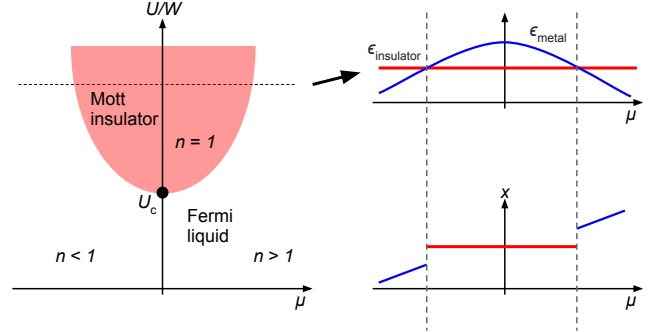


FIG. 1. The phase diagram for the Mott transition, plotted as a function of interaction strength  $U$  and chemical potential  $\mu$ . The energy vs.  $\mu$  curve at constant  $U$  exhibits level crossings between the metallic and insulating states. The discontinuity in the derivative  $x = -\partial\epsilon/\partial\mu$  implies thermodynamically forbidden densities where the system will phase separate into undoped  $x = 0$  and critically-doped  $x = x_c$  patches.

in experiment), we can explicitly write down the energy densities  $\epsilon = E/V$  for the metallic and insulating states, since the two states must independently exist over a finite parameter range and cross at the first-order transition. We determine the phase boundary of the Mott transition in the  $\mu$ - $U$  plane ( $\mu$  is chemical potential) and compute the scaling of the critical doping  $x_c$  with  $U$ .

Consider a one-band Hubbard model on generic lattice. The  $\mu$ - $U$  phase diagram generically consists of two regions: a Mott insulator occupying a finite range in  $\mu$  at sufficiently large  $U > U_c$ , and a Fermi liquid (actually a superconductor or any other compressible phase including a possible non-Fermi liquid will suffice for the argument) everywhere else (Fig. 1). Expanding the grand-canonical energy densities of the metal and insulator to lowest order about the bandwidth-controlled transition point (dot in labeled  $U_c$  in Fig. 1), we obtain:

$$\epsilon_m(\mu, U) = \epsilon_0 + d_m \Delta U - \frac{1}{2} \kappa (\Delta\mu)^2 \quad (1)$$

$$\epsilon_i(\mu, U) = \epsilon_0 + d_i \Delta U. \quad (2)$$

Here,  $\kappa = \partial x / \partial \mu$  is the electronic compressibility, where the doping  $x = n - 1$  is defined relative to half-filling, and

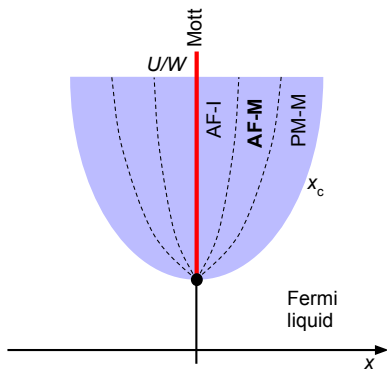


FIG. 2. Generic Mott phase diagram for a 3D system plotted in the  $U$ -vs- $x$  plane. Beginning at the pure Mott insulating state at zero doping  $x = 0$ , we progress through three phase-separated states (shaded) to arrive at a uniform Fermi liquid. The three phase-separated states have distinct magnetic (AF or PM) and transport (M or I) signatures. Since the percolation threshold  $\phi_c^{3D} \sim 1/3$ , we expect an intermediate phase (AF-M, bolded text) where metallic conductivity coexists with magnetic order. This intermediate phase is absent in 2D since  $\phi_c^{2D} \sim 1/2$ , so the metal and insulator are never simultaneously percolated.

$d_m$  and  $d_i$  are the per-site double-occupancies  $\langle n_{i\uparrow}n_{i\downarrow} \rangle$  in the metallic and insulating states. The chemical potential  $\Delta\mu = \mu - \mu_{n=1}$  and Coulomb repulsion  $\Delta U = U - U_c$  are measured relative to the bandwidth-controlled transition point.

Equating the two energies, we obtain the Mott phase boundary,

$$\Delta U = \frac{\Delta\mu^2}{2} \frac{\kappa}{d_m - d_i}. \quad (3)$$

The quadratic dependence  $U \sim \mu^2$  is observed within DMFT [14]. Evaluating the metallic density  $x = -\partial\epsilon/\partial\mu$  along the phase boundary, we obtain the critical doping

$$x_c = \sqrt{\Delta U \cdot 2\kappa(d_m - d_i)}. \quad (4)$$

Similar to the liquid-gas transition, thermodynamics forbids charge densities lying in the range  $0 < |x| < x_c$ . The system will phase separate if doped to lie within this regime [20].

We note that the filling-controlled transition is not doping in the conventional sense, where the insulator is connected to a metal formed by shifting  $\mu$  into the bands lying adjacent to the spectral gap. Indeed the smallness of  $\Delta\mu$  for small  $\Delta U$  implied by Eq. (3) dictates that the first order transition occurs without the closing of the single-particle gap, when  $\Delta U$  is small. Rather, the Mott insulator transitions to a disconnected, lower-energy, metallic state [11].

*Phase separation* – Thermodynamics forbids charge densities in the range  $0 < |x| < x_c$ , causing the system to phase separate into insulating regions with  $x = 0$  and

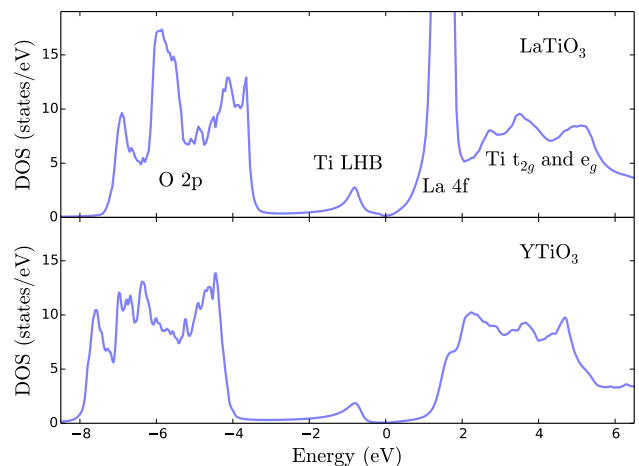


FIG. 3. Density of states for end members  $\text{LaTiO}_3$  and  $\text{YTiO}_3$  of the  $R\text{TiO}_3$  series computed using DFT+DMFT. The reduction of bandwidth in  $\text{YTiO}_3$  enhances the relative strength of correlations and produces a larger spectral gap. We emphasize that a single set of Coulomb parameters were used for both simulations, and the differences are driven purely by chemistry.

metallic regions with  $x = x_c$  (shaded region in Fig. 2). The surface energy  $E_{\text{surface}} \sim \sigma L^{d-1}$ , where  $\sigma > 0$  is the surface tension and  $L$  is the characteristic size of a metallic region, favors forming a single large puddle. However, the long-ranged part of the Coulomb interaction  $E_{\text{coul}} \sim x_c^2 L^{2d-1}$  penalizes macroscopic charge imbalances. Balancing the two gives domains of typical size  $L \sim (\sigma/x_c^2)^{1/d}$ . The actual spatial patterns formed depend on system-specific details such as dimensionality, anisotropy, and elastic forces [22].

Conducting transport does not coincide with the disappearance of phase separation at  $x_c$  and the formation of the homogeneous metallic state, but rather when the volume fraction  $x/x_c \sim \phi$  of the metallic puddles reaches the percolation limit, roughly  $\phi_c \sim 1/3$  in three dimensions [27]. Depending on the spatial patterns favored, we may expect anisotropic transport. Additionally, we predict an intermediate conducting magnetic state (AF-M in Fig. 2) since long-range order persists as long as the insulating regions percolate, up to doping  $x/x_c \sim 1 - \phi_c$ . This intermediate state does not exist in two dimensions since  $\phi_c \sim 1/2$ , implying the metallic and insulating states never simultaneously percolate.

*Ab initio modeling* – The rare earth titanates  $R\text{TiO}_3$  are an ideal system to investigate the Mott transition [25, 26]. Varying the ionic radius of the rare earth  $R$  tunes the correlation strength, while rare earth vacancies [28] or Ca substitution [6] tunes the Ti valence from  $d^1$  to  $d^0$ . The interplay between structure, transport and magnetism are well-characterized. Critical dopings, determined via transport, range from 0.05 in  $\text{LaTiO}_3$  to

0.35 in  $\text{YTiO}_3$ , and the predicted intermediate metallic antiferromagnetic state has been observed [6], although the claim is not without controversy [29]. Careful bulk measurements suggest signatures of phase separation [30, 31]. However, these prior studies suffer from chemical disorder due to the divalent substitution used to obtain filling control, so recent synthesis of high-quality electrostatically-doped heterostructures opens the possibility of filling-control without cation disorder [32].

To apply our theory to the titanates, we perform electronic structure calculations using the combination of density functional theory and dynamical mean-field theory [24] with the implementation described in Ref. 33. We used  $U = 9.0$  eV and  $J = 0.8$  eV for the strength of the Coulomb repulsion on the Ti  $t_{2g}$  orbitals, and  $E_{\text{dc}} = U(n_d - 1/2) - J(n_d - 1)/2$  with  $n_d = 1.0$  as the standard double-counting energy. The empty  $e_g$  orbitals do not require correlations for their correct description. We include all the valence states, notably the oxygen  $2p$  states in the hybridization window. We use  $T = 100$  K, well below the Mott transition temperature at half-filling. The value for  $U$  was determined by requiring the calculated gap of the end-member  $\text{LaTiO}_3$  to match the experimentally-determined value, reported to be in the range 20 meV to 0.2 eV [34]. Once fixed, these parameters were used to for the entire  $\text{RTiO}_3$  family. To capture correlations in the  $4f$  shells of the compounds with partially-filled rare earth ions, we applied the atomic self-energy

$$\Sigma_f(i\omega_n) = \Sigma_0 + \frac{U_f^2 p(1-p)}{i\omega_n + \mu - U_f(p - 1/2)}, \quad (5)$$

with the static shift  $\Sigma_0 = -U_f(p - 1/2) - \epsilon_f$ . Here,  $U_f = 10$  eV is the Hartree term on the  $f$ -shell,  $\epsilon_f$  is the center of mass of the  $f$  density of states, and  $p$  is the filling fraction (e.g.  $3/14$  for  $\text{NdTiO}_3$ ). Since the chemical potential is the independent variable in the scans needed to compute the  $n$  vs.  $\mu$  curves, we do not update the charge-density, as this would have required self-consistent adjustment of the nuclear charges. To obtain spectral quantities, we analytically continued the  $3d$  self-energy  $\Sigma$  onto the real axis by applying the maximum entropy method to the effective Green's function  $G = 1/(i\omega_n - E - \Sigma(i\omega_n))$ .

Shown in Fig. 3 is the density of states for the end-compounds  $\text{LaTiO}_3$  and  $\text{YTiO}_3$ . The contraction of the cation ionic radii from La to Y enhances the octahedral distortions, reducing the bandwidth of  $\text{YTiO}_3$  relative to  $\text{LaTiO}_3$  (observed within DFT). The reduction places the  $\text{YTiO}_3$  deeper inside the Mott insulating state, which is reflected in the increased spectral gap of nearly 2 eV. The salient features—the location of the lower Hubbard band and oxygen  $2p$  binding energies—agree well with photoemission [35, 36].

We explicitly determine the critical doping  $x_c$  of the titanates by monitoring the charge density as we lower

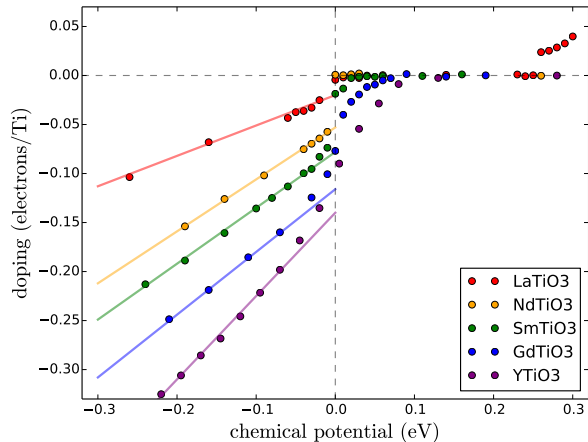


FIG. 4. Doping as a function of chemical potential near the hole-doped Mott transition, computed with DFT+DMFT for representative members of the  $\text{RTiO}_3$  family. The size of the density discontinuity (the critical doping  $x_c$ ) increases as we progress away from the the largest rare earth La. The lines are guides to the eye. The electron-doped transition can be seen for  $\text{LaTiO}_3$  in the upper right.

the chemical potential to hole-dope the Mott insulator (Fig. 4). The critical doping, as given by the discontinuity between the insulator and Fermi liquid, increases monotonically from  $\sim 2\%$  for La to  $\sim 15\%$  for Y, corroborating our expectation that correlations increase  $x_c$ . We note that the small contribution to the compressibility due to the partially-filled  $4f$  shells for the intermediate rare earths has been subtracted out to give a flat  $n$  vs.  $\mu$  curve in the Mott insulating regime. We do not observe a jump in  $\text{GdTiO}_3$  and  $\text{YTiO}_3$  because the Mott critical endpoint drops below the simulation temperature of  $T = 100$  K, as observed experimentally [6], so we roughly extract  $x_c$  by pinpointing the location of steepest slope in the  $n$  vs.  $\mu$  curve. The critical dopings are smaller than experiment a factor of 2, which we attribute to the effect the strong chemical disorder required for doping, as well as polarons, which is known to drive the finite- $T$  Mott transition more strongly first-order [37].

As a consistency check, we also determine  $x_c$  for representative compounds using Eq. 4, which is valid near bandwidth-controlled transition point. First, we determined the critical Coulomb strengths  $U_c$  for the bandwidth-controlled transition, which decrease from  $\text{LaTiO}_3$  to  $\text{YTiO}_3$  as expected. The charge compressibility was obtained by scanning  $n$  vs.  $\mu$  at  $U_c$ . To obtain the “double-occupancy” of the metallic and insulating solutions, we note that in multiband models, the Coulomb  $U$  couples to the generalization of the on-site double-occupancies—the Hartree component of the potential energy— $N_i(N_i - 1)/2$  where  $N_i$  runs from 0 to 10 within the  $3d$  manifold. The extracted parameters

Compound	$\kappa$ (e/eV)	$d_m$	$d_i$	$U_c$ (eV)	$x_c$
LaTiO <sub>3</sub>	0.20	0.15	0.13	8.8	4%
SmTiO <sub>3</sub>	0.22	0.22	0.19	6.0	20%
YTiO <sub>3</sub>	0.28	0.23	0.20	4.7	27%

TABLE I. For representative titanates, we tabulate the electronic compressibility per Ti atom  $\kappa = \partial n / \partial \mu$ , Hartree component of the potential energy  $d_{m,i} = \langle N(N-1)/2 \rangle$  in the metallic and insulating states, and the critical Coulomb strengths  $U_c$ . Using  $\Delta U = U - U_c$  where  $U = 9$  eV in our calculations, and Eq. 4, we compute the critical doping  $x_c$ .

are shown in Table. I. Again,  $x_c$  increases as we progress from the least- to the most-correlated compounds and roughly agree with those from the  $n$  vs.  $\mu$  curves, even for YTiO<sub>3</sub> which is quite far from the bandwidth-controlled transition.

*Summary* – We have outlined a theory for the first-order filling-controlled Mott transition, which predicts intrinsic electronic phase separation when a Mott insulator is doped away from half-filling, and demonstrated explicitly how to calculate the critical doping  $x_c$  in electronic structure calculations. The thermodynamic signatures of this pervasive phase-separation has been observed in many other correlated systems [1], as well as directly using near-field optics on VO<sub>2</sub> [38] and STM in the cuprates [39]. The key tasks to enhance the quantitative agreement between theory and experiment involve (a) including disorder and polarons into theoretical calculations, and (b) designing cleaner experimental systems where chemical disorder can be reduced, e.g. through modulation-doped samples or oxide heterostructures. The accessibility of thin films to spatially resolved probes (STM, spatially-resolved optics) is especially advantageous as they would allow direct visualization of the phase separated region.

C.Y. was supported by the Army Research Office MURI grant W911-NF-09-1-0398. L.B. was supported by the MRSEC Program of the National Science Foundation under Award No. DMR 1121053. We benefitted from facilities of the KITP, funded by NSF grant PHY-11-25915. We also acknowledge support from the Center for Scientific Computing at the CNSI and MRL: an NSF MRSEC (DMR-1121053) and NSF CNS-0960316.

\* cyee@kitp.ucsb.edu

- [1] M. Imada, A. Fujimori, and Y. Tokura, *Reviews of Modern Physics* **70**, 1039 (1998).  
 [2] P. Fazekas, *Lecture Notes on Electron Correlation and Magnetism*, Series in Modern Condensed Matter Physics, Vol. 5 (World Scientific Publishing Co. Pte. Ltd., 1999).  
 [3] a. Fujimori, *Journal of Physics and Chemistry of Solids* **53**, 1595 (1992).  
 [4] P.-H. Xiang, S. Asanuma, H. Yamada, I. H. Inoue,

- H. Akoh, and a. Sawa, *Applied Physics Letters* **97**, 032114 (2010).  
 [5] A. a. Belik, R. V. Shpanchenko, and E. Takayama-Muromachi, *Journal of Magnetism and Magnetic Materials* **310**, e240 (2007).  
 [6] T. Katsufuji, Y. Taguchi, and Y. Tokura, *Physical Review B* **56**, 10145 (1997).  
 [7] H. Kajueter, G. Kotliar, and G. Moeller, *Physical review. B, Condensed matter* **53**, 16214 (1996).  
 [8] P. A. Lee, N. Nagaosa, and X.-G. Wen, *Reviews of Modern Physics* **78**, 17 (2006).  
 [9] G. Kotliar and A. E. Ruckenstein, *Physical Review Letters* **57**, 1362 (1986).  
 [10] S. Onoda and M. Imada, *Journal of the Physical Society of Japan* **70**, 3398 (2001).  
 [11] M. Balzer, B. Kyung, D. Sénéchal, A.-M. S. Tremblay, and M. Pothoff, *EPL (Europhysics Letters)* **85**, 17002 (2009).  
 [12] T. Misawa and M. Imada, , 16 (2013), arXiv:1306.1434.  
 [13] A. Georges, G. Kotliar, W. Krauth, and M. J. Rozenberg, *Reviews of Modern Physics* **68**, 13 (1996).  
 [14] P. Werner and A. Millis, *Physical Review B* **75**, 085108 (2007).  
 [15] N. Furukawa and M. Imada, *Journal of the Physical Society of Japan* **61**, 3331 (1992).  
 [16] P. Visscher, *Physical Review B* **10**, 943 (1974).  
 [17] V. Emery, S. Kivelson, and H. Lin, *Physical Review Letters* **64**, 475 (1990).  
 [18] W. Putikka and M. Luchini, *Physical Review B* **62**, 1684 (2000).  
 [19] S. White and D. Scalapino, *Physical Review B* **61**, 6320 (2000).  
 [20] D. Galanakis, E. Khatami, K. Mikelsons, a. Macridin, J. Moreno, D. a. Browne, and M. Jarrell, *Philosophical transactions. Series A, Mathematical, physical, and engineering sciences* **369**, 1670 (2011).  
 [21] B. Spivak and S. a. Kivelson, *Annals of Physics* **321**, 2071 (2006).  
 [22] C. Ortix, J. Lorenzana, and C. Di Castro, *Physica B: Condensed Matter* **404**, 499 (2009).  
 [23] A. Giuliani, J. L. Lebowitz, and E. H. Lieb, *Physical Review B* **84**, 064205 (2011).  
 [24] G. Kotliar, S. Savrasov, K. Haule, V. Oudovenko, O. Parcollet, and C. Marianetti, *Reviews of Modern Physics* **78**, 865 (2006).  
 [25] J. Greedan, *Journal of the Less Common Metals* **111**, 335 (1985).  
 [26] M. Mochizuki and M. Imada, *New Journal of Physics* **6**, 154 (2004).  
 [27] J. Essam, *Reports on Progress in Physics* **43** (1980).  
 [28] A. Sefat, J. Greedan, and L. Cranswick, *Physical Review B* **74**, 104418 (2006).  
 [29] A. Sefat, J. Greedan, G. Luke, M. Niéwczas, J. Garrett, H. Dabkowska, and A. Dabkowski, *Physical Review B* **74**, 104419 (2006).  
 [30] C. Hays, J.-S. Zhou, J. Markert, and J. Goodenough, *Physical Review B* **60**, 10367 (1999).  
 [31] H. Zhou and J. Goodenough, *Physical Review B* **71**, 165119 (2005).  
 [32] P. Moetakef, T. a. Cain, D. G. Ouellette, J. Y. Zhang, D. O. Klenov, A. Janotti, C. G. Van de Walle, S. Rajan, S. J. Allen, and S. Stemmer, *Applied Physics Letters* **99**, 232116 (2011).  
 [33] K. Haule, C.-H. Yee, and K. Kim, *Physical Review B*

- [81](#), 1 (2010).
- [34] P. Lunkenheimer, T. Rudolf, J. Hemberger, a. Pimenov, S. Tachos, F. Lichtenberg, and a. Loidl, [Physical Review B](#) **68**, 245108 (2003).
- [35] A. Fujimori, I. Hase, M. Nakamura, H. Namatame, Y. Fujishima, Y. Tokura, M. Abbate, F. de Groot, M. Czyzyk, J. Fuggle, O. Strebel, F. Lopez, M. Domke, and G. Kaindl, [Physical Review B](#) **46**, 9841 (1992).
- [36] A. Fujimori, I. Hase, H. Namatame, Y. Fujishima, Y. Tokura, K. Takegahara, and F. M. F. de Groot, [Physical Review Letters](#) **69**, 1796 (1992).
- [37] M. Capone, G. Sangiovanni, C. Castellani, C. Di Castro, and M. Grilli, [Physical Review Letters](#) **92**, 106401 (2004).
- [38] M. M. Qazilbash, M. Brehm, B.-G. Chae, P.-C. Ho, G. O. Andreev, B.-J. Kim, S. J. Yun, A. V. Balatsky, M. B. Maple, F. Keilmann, H.-T. Kim, and D. N. Basov, [Science \(New York, N.Y.\)](#) **318**, 1750 (2007).
- [39] Y. Kohsaka, T. Hanaguri, M. Azuma, M. Takano, J. C. Davis, and H. Takagi, [Nature Physics](#) **8**, 1 (2012).